

CBQ: Cross-Block Quantization for Large Language Models

Xin Ding ^{*1,2} Xiaoyu Liu ^{*1,2} Zhijun Tu ² Yun Zhang ^{2,3} Wei Li ² Jie Hu ² Hanting Chen ² Yehui Tang ²
Zhiwei Xiong ¹ Baoqun Yin ¹ Yunhe Wang ²

Abstract

Post-training quantization (PTQ) has played a key role in compressing large language models (LLMs) with ultra-low costs. However, existing PTQ methods only focus on handling the outliers within one layer or one block, which ignores the dependency of blocks and leads to severe performance degradation in low-bit settings. In this paper, we propose CBQ, a cross-block reconstruction-based PTQ method for LLMs. CBQ employs a cross-block dependency using a homologous reconstruction scheme, establishing long-range dependencies across multiple blocks to minimize error accumulation. Furthermore, CBQ incorporates a coarse-to-fine preprocessing (CFP) strategy for suppressing weight and activation outliers, coupled with an adaptive LoRA-Rounding technique for precise weight quantization. These innovations enable CBQ to not only handle extreme outliers effectively but also improve overall quantization accuracy. Extensive experiments show that CBQ achieves superior low-bit quantization (W4A4, W4A8, W2A16) and outperforms existing state-of-the-art methods across various LLMs and datasets. Notably, CBQ quantizes the 4-bit LLAMA1-65B model within only 4.3 hours on a single GPU, achieving a commendable tradeoff between performance and quantization efficiency.

1. Introduction

Large language models (LLMs) (Wei et al., 2022a; Radford et al.; Zhang et al.; Brown et al., 2020), have sparked

^{*}Equal contribution ({xinding64, liuxyu}@mail.ustc.edu.cn);
This work was done during Xin Ding and Xiaoyu Liu's internship at Huawei Noah's Ark Lab. ¹University of Science and Technology of China ²Huawei Noah's Ark Lab ³DSA Thrust, INFO Hub, Hong Kong University of Science and Technology (GZ). Correspondence to: Yunhe Wang <yunhe.wang@huawei.com>, Baoqun Yin <bqyin@ustc.edu.cn>.

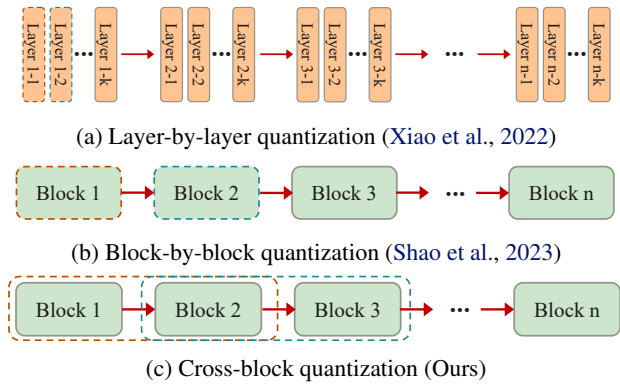


Figure 1. Comparison of different optimization manners in post-training quantization for large language models. Orange and blue dashed boxes indicate the order of quantization optimization.

immense academic and industrial interest owing to their remarkable performance in handling complex natural languages tasks (Hendrycks et al., 2020b; Bisk et al., 2020b), like language generation, translation, question answering, and text summarization *etc.* However, the sheer size of these models, often comprising billion-level parameters, demands significant computational resources for inference and deployment. This problem necessitates the employment of model compression techniques such as network pruning (Han et al., 2015), knowledge distillation (Hinton et al., 2015), network quantization (Choi et al., 2018; Frantar et al., 2022b), and neural architecture search (Zoph & Le, 2016) *etc.* Compared with most compression methods that require huge training costs and access to complete training data, the post-training quantization (PTQ) technique (Frantar et al., 2022a; Lin et al., 2023; Xiao et al., 2022; Wei et al., 2023) operating with limited calibration data and computational resources is more in demand for compressing LLMs.

Previous PTQ methods (Wei et al., 2023; Xiao et al., 2022; Shao et al., 2023) for LLMs mainly focus on designing accurate outliers suppression schemes for floating-point activations, and then conduct quantization with vanilla policy. They locate the position and optimize the channel scale of activations with outliers in a layer-by-layer or block-by-block manner, as shown in Fig. 1. However, these methods lead to accumulated errors and sub-optimal quantization

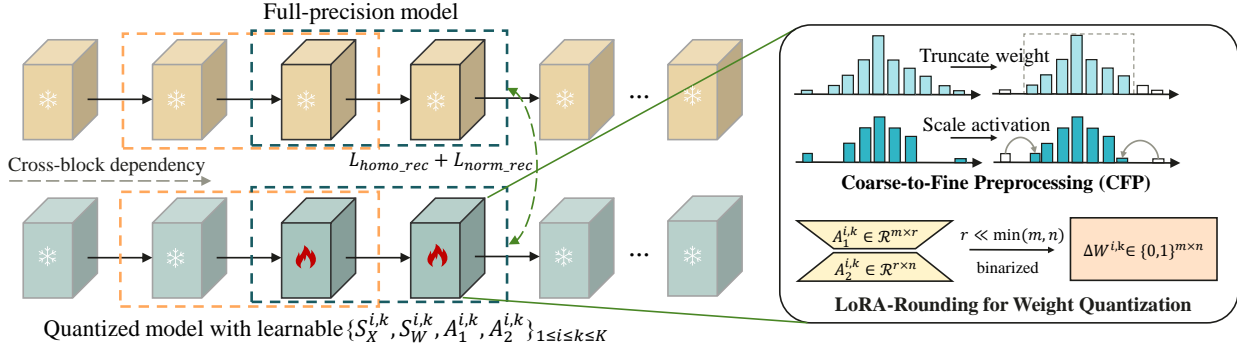


Figure 2. Workflow of the proposed CBQ. CBQ firstly utilizes a coarse-to-fine preprocessing to handle the outliers of weights and activations, and then employs a cross-block optimization strategy to learn quantization step sizes and weight adaptive rounding matrices with supervision from the corresponding full-precision model. This sequential block-wise method minimizes aggregate error propagation through cross-block dependency modeling.

across the entire model for not taking the dependency across blocks into consideration. Moreover, these PTQ methods suffer from the absence of joint optimization for reducing quantization errors of weights and activations, resulting in significant performance degradation when compressing LLMs into low-bit settings, such as W2A16 and W4A4.

In this paper, we present CBQ, a comprehensive PTQ solution tailored for LLMs, which incorporates outlier suppression, learnable quantization step sizes, and adaptive rounding in a unified cross-block framework, as shown in Fig. 2. CBQ introduces a cross-block dependency (CBD) into block-wise reconstruction, helping mitigate the issue of accumulated errors across the entire model. Our approach ensures that multiple transformer blocks within a sliding window with overlapping are optimized simultaneously. This overlapping window mechanism, complemented by a novel homologous reconstruction scheme, allows for more effective and non-local optimization of quantization parameters. To reduce reconstruction difficulties posed by extreme weight and activation outliers, CBQ incorporates a novel coarse-to-fine preprocessing (CFP) strategy. CFP utilizes a quartile criterion to coarsely determine the range of outliers and then precisely pinpoint the locations of the outliers based on feature distributions. Then we truncate weight outliers and perform equivalent scaling on the activation outliers. Furthermore, CBQ introduces a LoRA-Rounding technique, employing two low-rank matrices to learn the adaptive rounding values for quantized weight, which helps rectify weight quantization errors while preserving training efficiency. It is worth noting that the step sizes of weights and activations, and the rounding matrices are jointly optimized in our proposed quantization framework. CBQ’s innovative approach in cross-block reconstruction, advanced outlier processing, and adaptive rounding establish it as a groundbreaking solution in the field of PTQ for LLMs.

The contributions of this paper are summarized as follows:

- We propose a unified PTQ method tailored to LLMs based on cross-block reconstruction, which introduces a cross-block dependency mechanism to reduce accumulated errors in a block-wise manner.
- We design a coarse-to-fine pre-processing strategy to truncate weight outliers and equivalently scale activation outliers to reduce the reconstruction difficulty.
- We present LoRA-Rounding, an efficient adaptive rounding scheme that optimizes rounding errors of weight quantization via two low-rank matrices.
- Extensive experiments demonstrate that CBQ achieves low-bit quantization settings such as W4A4, W4A8, and W2A16, and outperforms state-of-the-art methods across various models and benchmark datasets.

2. Related works

Post-training quantization. The post-training quantization (PTQ) algorithm (Nagel et al., 2021) converts the pre-trained full-precision network into a fixed-point network with a few unlabeled calibration data and computational overhead, which enables fast deployment on various devices. Recent post-training quantization methods have been widely explored in vision models (Liu et al., 2021; Hubara et al., 2021; Frantar & Alistarh, 2022; Cai et al., 2020). Some techniques like AdaQuant (Hubara et al., 2020), AdaRound (Nagel et al., 2020), and BRECQ (Li et al., 2021) minimize the distance between floating point and quantized model outputs to optimize quantization parameters. While BRECQ incorporates Fisher information and jointly optimizes layers within each residual block, it still obtains sub-optimal performance for not capturing interactions across neighboring residual blocks. The proposed CBQ improves quantization accuracy that accounts for dependencies between adjacent blocks.

Quantization for large language models. Existing large language models such as BLOOM (Laurenc̄on et al., 2022), OPT (Zhang et al., 2022), and LLAMA (Touvron et al.) contain tens of billions of parameters, and require massive memory footprint and computation requirements in the inference. Recent works have been proposed to compress LLMs with post-training quantization methods that do not require a complete training procedure and access to a full training dataset. LLM.int8() (Dettmers et al.), ZeroQuant (Yao et al., 2022) and nuQmm (Park et al., 2022) focus on quantizing the parameters with mixed-precision decomposition scheme, representing the outliers with 16-bit and others with 8-bit. These methods can not truly accelerate the inference of LLMs for that is hard to implement on hardware. Other methods like GPTQ (Frantar et al., 2022b) and AWQ (Lin et al., 2023) can efficiently quantize LLMs but they focus on FP16 activations and INT4 weights, which can not benefit from the integer matrix multiplication of existing AI accelerators. Additionally, Some methods like SmoothQuant (Xiao et al., 2022), Outlier Suppression (Wei et al., 2022b), Outlier Suppression+ (Wei et al., 2023) and QLLM (Liu et al., 2023) aim at processing activation outliers and lack optimization for the weight quantization. Moreover, these methods rely on hand-craft quantization strategies which are tuned based on extensive experimentation for optimization. Recent block reconstruction-based PTQ method OmniQuant (Shao et al., 2023), suffers from error accumulation from the lack of cross-block dependency. In contrast, CBQ incorporates outlier suppression, learnable step sizes, and adaptive rounding in a unified cross-block framework, which enables efficient and high-performance quantization for LLMs.

3. Methods

In this section, we introduce the proposed cross-block quantization framework tailored to LLMs. As illustrated in Fig. 2, CBQ firstly handles the outliers of weights and activations, and then jointly learns step sizes of weights and activations and weight-rounding matrices in a cross-block manner. CBQ reconstructs the output feature of the last block in each sliding window based on the corresponding supervision of the full-precision model.

We first give a brief introduction to quantization, which aims to represent weights and activations of float model with lower bit-width for reducing the memory and computational cost. Given floating-point weights W and activations X , the k -bit quantized and de-quantized processing of weights and activations can be represented as

$$Q(X) = S_X \cdot \left\lfloor \frac{X}{S_X} \right\rfloor; \quad Q(W) = S_W \cdot \left(\left\lfloor \frac{W}{S_W} \right\rfloor + \Delta_W \right), \quad (1)$$

where $Q(\cdot)$ is an uniform quantizer, S_X and S_W are the quantization step sizes of activations and weights. $\lfloor \cdot \rfloor$ and

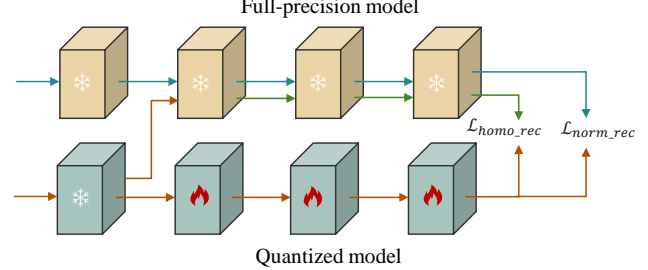


Figure 3. Diagram of the homologous reconstruction scheme. \mathcal{L}_{homo_rec} and \mathcal{L}_{norm_rec} represent the homologous reconstruction loss and the normal reconstruction loss, respectively.

$\lfloor \cdot \rfloor$ represent rounding to the nearest integer and rounding towards negative infinity, respectively. Δ_W denotes the quantization rounding matrix for weight, where each element belongs to $\{0, 1\}$. For simplicity, we omit the offset and clipping operation in Eq. 1.

3.1. Cross-block reconstruction

Most existing post-training quantization methods (Xiao et al., 2022; Lin et al., 2023; Wei et al., 2023; Frantar et al., 2022a) for LLMs conduct calibration in a layer-wise manner, optimizing the quantization step sizes of weights and inputs, respectively. OmniQuant (Shao et al., 2023) adopts a learnable method in a block-wise manner but ignores the issue of accumulated errors across the entire model. Besides, previous quantization methods get the rounding values of weights based on the policy of rounding to the nearest integer value, which is not the best for it not adapts to the data and the task loss (Nagel et al., 2020). In this paper, we propose to jointly optimize the step sizes and weight rounding values (S_X , S_W and Δ_W) in a unified cross-block framework. For a large language model with K transformer blocks, the objective for joint optimization of the quantization parameters within k^{th} block is formulated as

$$\arg \min_{S_X^k, S_W^k, \Delta_W^k} \mathbb{E}(T_k(W^k, X^k), T_k(Q(W^k), Q(X^k)), \quad (2)$$

where $1 \leq k \leq K$, $T(\cdot)$ is a transformer block, W^k and X^k are weights and activations within the k^{th} block, respectively. S_X^k and S_W^k are quantization step sizes of activation and weight quantization in the block, respectively, which are learnable during optimization. And $\mathbb{E}(\cdot)$ represents the metric to evaluate the reconstruction errors between outputs of quantized block and full-precision block.

Cross-block dependency. While block-wise reconstruction is effective in saving computational memory, it only considers the local information within each block, neglecting the dependency across different blocks. The reconstruction error will accumulate as the stack of transformer blocks, incurring suboptimal solutions for quantization parameters

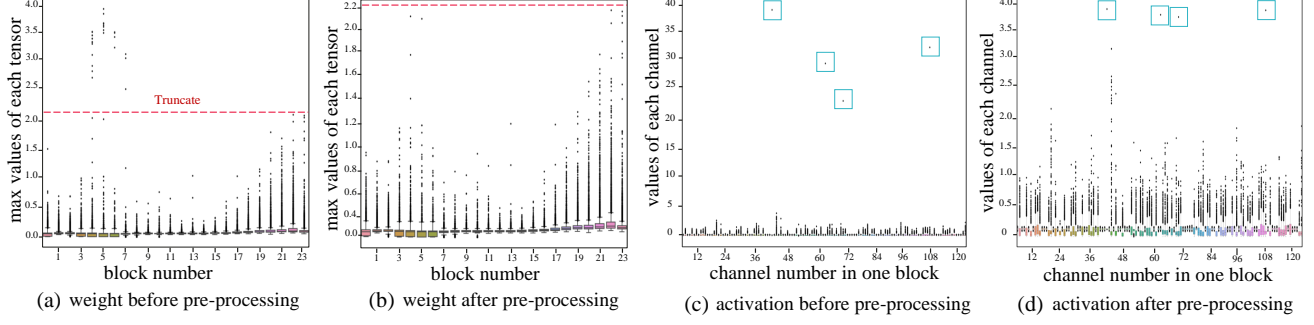


Figure 4. Outliers pre-processing for weights and activations. The red dashed line indicates the truncation threshold for weight outliers, and the deep blue line represents the reserved subset. The light blue boxes depict activation outliers that undergo per-channel scaling.

To tackle this issue, we introduce a cross-block dependency (CBD) scheme using a sliding window approach. This scheme enables the simultaneous optimization of multiple blocks within the window. Furthermore, the two adjacent sliding windows have overlapping blocks, ensuring that the blocks between the windows are also interconnected. The CBD scheme enhances the connectivity and cooperation between blocks, enabling them to jointly contribute to the quantization process. This holistic optimization strategy leads to better overall performance and addresses the limitations of block-wise reconstruction in capturing cross-block dependencies. We formulate the optimization with the CBD scheme as

$$\arg \min_{S_X^{i,k}, S_W^{i,k}, \Delta_W^{i,k}} \mathbb{E}(T_{i,k}(W^{i,k}, X^{i,k}), T_{i,k}(Q(W^{i,k}), Q(X^{i,k})), \quad (3)$$

where $1 \leq i \leq k \leq K$, $T_{i,k}$ represents the blocks from block i to block k within one sliding window, and the same applies to the symbols $S_X^{i,k}$, $S_W^{i,k}$ and $\Delta_W^{i,k}$.

Although the CBD technique helps reduce the reconstruction difficulty, it is important to note that it cannot completely eliminate the accumulated errors and the optimization within each window remains local. To address this limitation and further enhance the reconstruction process while ensuring stability, we introduce an additional homologous reconstruction scheme, as illustrated in Fig. 3. In this scheme, we input the output of the previous block of the quantized model into the current block of the full-precision model. This generates an additional output that is homologous to the outputs of the quantized model. By minimizing the reconstruction errors between these two homologous outputs, CBD could help improve the overall accuracy and stability of the reconstruction process. Additionally, the optimization object is the average of the homologous reconstruction error $\mathcal{L}_{homologous}$ and the normal reconstruction

error \mathcal{L}_{norm_rec} :

$$\mathcal{L}_{rec} = \underbrace{\mathbb{E}(T_{i,k}(W^{i,k}, X^{i,k}), T_{i,k}(Q(W^{i,k}), Q(X^{i,k}))}_{\mathcal{L}_{norm_rec}} + \underbrace{\mathbb{E}(T_{i,k}(W^{i,k}, Q(X^{i,k})), T_{i,k}(Q(W^{i,k}), Q(X^{i,k}))}_{\mathcal{L}_{homologous}}. \quad (4)$$

For the distance metric, we incorporate \mathcal{L}_2 and Kullback-Leibler divergence (KLD) loss (Kullback & Leibler, 1951) to measure reconstruction error. KLD computes the likelihood distribution between output features that undergo the softmax function. It tends to suppress outliers in the feature space and enhance the robustness of the optimization process. By incorporating both terms, our method captures both the spatial distance and the distribution discrepancy, leading to a more comprehensive and robust optimization process. Then the distance metric is formulated as:

$$\mathbb{E}(h_1, h_2) = ||h_1 - h_2||_2 + D_{KL}(\sigma(h_1), \sigma(h_2)), \quad (5)$$

where h_1 and h_2 are hidden states from the outputs of full-precision blocks and quantized blocks, respectively. σ is the softmax function. $||\cdot||_2$ represents the \mathcal{L}_2 distance and $D_{KL}(\cdot)$ represents the KLD distance. We provide the ablation study on the loss functions in Table 6.

3.2. Coarse-to-fine pre-processing

To address the challenges in achieving optimal quantization parameters before cross-block reconstruction, we have conducted a thorough analysis of outliers in both weights and activations. Based on this analysis, we have developed an effective and unified design approach to handle extreme weight and activation outliers.

Figure 4 illustrates the block-by-block visualization of the weight distribution of the last fully connected layer, as well as the channel-by-channel visualization of the activation distribution within one block. It is observed that outliers in both weights and activations contribute to larger reconstruc-

Models	#Bits	Methods	PIQA	HellaSwag	ARC-C	ARC-E	Mutual	Ethics
OPT-30B	FP	-	78.18	72.27	38.14	65.40	69.72 / 48.83 / 74.98	60.28
	W4A16	GPTQ OmniQuant CBQ	78.10 78.06 78.36	71.50 71.29 72.23	37.54 37.98 38.06	63.88 65.19 65.35	68.64 / 47.40 / 74.27 69.34 / 48.64 / 74.71 69.77 / 49.32 / 74.47	58.64 58.73 61.31
	W4A8	OmniQuant RPTQ CBQ	77.20 76.93 78.26	71.17 71.25 71.55	37.11 37.45 37.89	64.60 63.46 64.92	68.81 / 47.51 / 74.60 68.98 / 47.67 / 74.75 69.01 / 47.72 / 74.81	59.17 59.21 59.23
	W4A4	OmniQuant CBQ	75.38 75.89	67.47 67.49	33.27 34.81	61.23 61.58	67.12 / 45.14 / 72.34 67.73 / 45.94 / 73.14	56.30 56.60
	FP	-	79.81	74.86	40.01	67.26	69.84 / 48.87 / 74.94	58.14
	W4A16	GPTQ OmniQuant CBQ	79.32 79.43 79.71	73.15 73.27 74.69	38.95 38.97 39.18	65.45 66.85 67.38	69.10 / 48.46 / 74.26 69.04 / 48.45 / 74.24 69.50 / 48.65 / 74.83	54.90 55.87 57.35
	W4A8	OmniQuant RPTQ CBQ	77.12 77.52 79.12	73.56 74.01 74.21	37.65 38.82 39.25	65.89 64.60 67.16	68.25 / 47.63 / 73.85 68.54 / 47.87 / 73.94 69.07 / 48.32 / 74.53	56.93 56.95 56.98
	W4A4	OmniQuant CBQ	77.85 78.01	71.76 72.34	37.20 37.56	63.29 63.78	68.20 / 46.61 / 73.02 68.76 / 47.20 / 73.56	55.54 55.82
OPT-66B	FP	-	80.09	79.21	45.39	58.92	72.45 / 53.49 / 78.21	57.42
	W4A16	GPTQ OmniQuant CBQ	79.62 79.83 80.12	78.81 78.95 79.11	44.54 46.26 46.65	58.42 59.34 59.89	72.30 / 52.93 / 77.44 72.29 / 53.38 / 77.65 72.85 / 53.95 / 78.56	56.30 56.21 57.85
	W2A16	GPTQ OmniQuant CBQ CBQ*	51.03 77.23 77.23 79.85	26.34 73.85 75.05 78.32	26.02 43.52 42.93 44.98	28.87 55.23 57.12 58.42	56.53 / 29.80 / 58.13 70.62 / 50.89 / 74.96 69.96 / 49.93 / 75.65 72.36 / 52.46 / 77.65	52.72 50.36 56.35 55.34
	W4A8	OmniQuant CBQ	78.95 79.34	76.34 78.98	44.62 45.13	57.36 58.45	71.03 / 52.89 / 77.06 71.35 / 53.23 / 77.64	57.05 57.19
	W4A4	OmniQuant QLLM CBQ	71.21 73.83 76.33	64.65 67.91 72.74	34.47 38.40 42.92	49.45 50.67 54.50	67.10 / 45.37 / 71.44 - 70.12 / 50.45 / 74.73	47.69 - 48.70
	FP	-	80.79	80.72	46.24	58.71	73.03 / 54.17 / 79.12	61.75
	W4A16	GPTQ OmniQuant CBQ	80.79 81.01 81.12	79.86 80.30 80.76	45.45 45.74 45.98	58.13 58.41 58.64	72.89 / 53.84 / 78.57 72.99 / 54.06 / 79.11 73.06 / 54.29 / 78.89	58.45 60.12 61.49
	W4A8	OmniQuant CBQ	79.21 79.95	78.96 79.30	44.63 45.43	57.68 58.12	72.24 / 53.89 / 78.65 72.83 / 54.27 / 79.02	59.68 61.25
LLAMA1-65B	W4A4	OmniQuant QLLM CBQ	71.81 73.56 77.69	66.81 70.94 76.65	35.92 39.68 43.25	48.02 52.06 56.01	68.49 / 47.29 / 73.70 - 70.93 / 51.35 / 75.62	57.19 - 57.50

Table 1. Evaluation on multiple zero-shot datasets with the accuracy \uparrow metric, where the Mutual dataset is evaluated with the Mean Reciprocal Rank/Recall@1/Recall@2 metrics. CBQ* represents that the experiments conducted with 2-bit weight-only quantization did not involve fully quantizing the model but only the FC2 layer of the first transformer block was converted to 4-bit precision.

tion errors between the quantized and full-precision models. To address this issue, we analyze the distribution of outliers and propose a coarse-to-fine pre-processing strategy to suppress outliers and reduce the difficulty of reconstruction.

Coarse-grained detection. The comprehensive algorithm of the outlier detection is illustrated in Algorithm 3.1, which is divided into two stages. In the first stage, we perform coarse-grained detection by calculating the lower and upper quartile values (Q_1 and Q_3) and the interquartile range (IQR) in the numerical distribution (either activations or weights). Based on these calculations, we obtain a coarse outlier set $O = \{x|x > T, x \in X\}$, where $T = Q_3 + \lambda_1 IQR$ and λ_1 is set to 1.5. This stage greatly reduces the search space for outlier detection.

Fine-grained detection. In the second stage, we perform fine-grained detection by searching for a threshold that splits the coarse outlier set into an outlier subset $O_{outlier}$ and a reserved subset $O_{reserved}$. The goal is to minimize the intra-set variance $M_{intra} = \text{Var}(O_{reserved})$ while maximizing the distance between the two subsets $M_{inter} = (\text{Min}(O_{outlier}) - \text{Max}(O_{reserved}))^2$. To balance these objectives, we define a metric $M = M_{inter} - \lambda_2 M_{intra}$, where $\lambda_2 = 1.0$. By minimizing this metric, we can effectively identify outliers and distinguish them from the remaining data.

Removing outliers in weights has minimal impact on performance, whereas outliers in activations, particularly in specific channels, can greatly affect performance if directly

Algorithm 1 Coarse-to-Fine Preprocessing

Input: The input tensor X ,
 The balancing coefficient λ_1, λ_2
Output: Outlier O

1 **Coarse-grained Detection:**

2 $X_{\text{sorted}} = \text{Sort}(X);$
 3 $Q_1 = X[n/4], Q_3 = X[3n/4];$
 4 $IQR = Q_3 - Q_1;$
 5 $T = Q_3 + \lambda_1 IQR;$
 6 $O = \{x | x > T, x \in X_{\text{sorted}}\};$
 7 { **Fine-grained Detection.**}
 8 $N = \text{Len}(O), M^* = \text{INF};$
 9 **foreach** $i = 0$ **to** N **do**

10 $O_{\text{outlier}} = O_{i:N};$
 11 $O_{\text{reserved}} = O_{0:i};$
 12 $M_{\text{intra}} = \text{Var}(O_{\text{reserved}});$
 13 $M_{\text{inter}} = (\text{Min}(O_{\text{outlier}}) - \text{Max}(O_{\text{reserved}}))^2;$
 14 $M = M_{\text{inter}} - \lambda_2 M_{\text{intra}};$
 15 **if** $M > M^*$ **then**
 16 $O^* = O_{\text{outlier}};$
 17 $M^* = M.$
 18 **end**
 19 **end**

removed. Consequently, our approach involves truncating weight outliers and scaling outliers in activations based on the detected outliers in both weights and activations. This is different from existing outlier pre-processing methods (Xiao et al., 2022; Wei et al., 2023) that focus solely on activations. Figure 4 provides visual evidence of weight outliers being truncated within the outlier group. Additionally, the figure demonstrates the presence of outliers in specific channels. Scaling these specific channels results in a significant concentration of the overall distribution.

The scaling factor s_i for the activation tensor in i^{th} channel (represented as X_i) is determined by the maximum absolute value of the truncated outlier set O^* :

$$s_i = \sqrt{\text{Max}(|X_i|) / \text{Max}(O^*)}. \quad (6)$$

This scaling factor is then applied to update weights and activations following prior work (Wei et al., 2023) to counteract destabilizing fluctuations from remaining outliers.

3.3. LoRA-Rounding for weight quantization

The performance degradation raised by weight quantization is non-negligible when compressing the model into low bit-width. The quantization error of weights comes from the rounding error (Nagel et al., 2020) and clipping error (Tu et al., 2021), but previous PTQ methods for LLMs only focus on the optimization of the latter one and do not take the rounding error into consideration. AdaRound (Nagel et al.,

#Bits	Methods	OPT-30B		OPT-66B		LLAMA1-30B		LLAMA1-65B	
		C4	Wiki	C4	Wiki	C4	Wiki	C4	Wiki
FP	-	10.69	9.56	10.28	9.34	5.98	4.10	5.62	3.53
W4A16	GPTQ	10.80	9.63	10.50	9.55	6.16	4.34	5.77	3.77
	OmniQ	10.80	9.71	10.63	9.37	6.06	4.19	5.68	3.62
	CBQ	10.73	9.65	10.31	9.41	6.03	4.14	5.62	3.59
W4A8	OmniQ	10.96	9.95	10.73	9.52	6.45	4.58	6.12	3.96
	RPTQ	11.01	10.22	10.57	9.46	-	-	-	-
	CBQ	10.86	9.83	10.42	9.44	6.25	4.32	5.96	3.84
W4A4	OmniQ	11.89	10.60	11.35	10.29	12.49	10.33	11.28	9.17
	QLLM	-	-	-	-	11.51	8.37	8.89	6.87
	CBQ	11.79	10.34	11.02	9.45	9.73	7.96	7.52	5.89

Table 2. Evaluation quantization on generation datasets with the perplexity (PPL) \downarrow metric, where OmniQ represents OmniQuant.

2020) introduces to learn a better weight-rounding matrix for post-training quantization that adapts to the data and the task loss. As shown in Eq. 7, we can obtain the weight-rounding matrix $\Delta_W \in \mathbb{R}^{d \times k}$ with a learnable matrix $V \in \mathbb{R}^{d \times k}$ with a rectified sigmoid function:

$$\Delta_W = \text{Clip}(\text{Sigmoid}(V)(\zeta - \gamma) + \gamma, 0, 1), \quad (7)$$

where ζ and γ are stretch parameters and are fixed to 1.1 and -0.1, and $\text{Clip}(\cdot)$ clamps the inputs into a given range. The size of the weight-rounding matrix Δ_W is the same as the original weights.

However, the technique of AdaRound is hard to apply directly to LLMs with billion-level parameters, which could lead to much computational overhead and significantly reduce the efficiency of post-training quantization. To further rectify weight quantization errors arising from rounding operations and prevent their accumulation in adjacent blocks, we introduce an efficient adaptive rounding method for LLMs, called LoRA-Rounding. Specifically, inspired by LoRA (Hu et al., 2021), we employ low-rank adaptive learning on the weight-rounding matrices, decomposing V with much smaller low-rank matrices, and only optimize them in post-training quantization, the decomposition is defined as:

$$V = A_1 \times A_2, A_1 \in \mathbb{R}^{d \times r}, A_2 \in \mathbb{R}^{r \times k}, \quad (8)$$

where the rank $r \ll \min(d, k)$. Following the setting of LoRA (Hu et al., 2021), we utilize a random Gaussian initialization for A_1 and zero for A_2 , thus Δ_W is set to zero at the beginning of post-training quantization. During training, each element of V is encouraged into 0 or 1 with a regularizer loss:

$$\mathcal{L}_{\text{round}} = \sum_{i,j} 1 - |2\Delta_W(i,j) - 1|^\beta, \quad (9)$$

where β is a annealing factor. Following AdaRound (Nagel et al., 2020), β is set to higher in the initial phase and set to lower in the later phase of the optimization to encourage it to converge to 0 or 1. We also conduct $\Delta_W = \lfloor \Delta_W \rceil$ in the

later phase of the optimization to force each element into $\{0, 1\}$ exactly.

Compared with vanilla AdaRound for LLMs. The proposed LoRA-Rounding reduces the number of learnable parameters from $d \times k$ to $(d + k) \times r$ and accelerates the optimization process significantly, we conduct ablation experiments in the next section.

Compared with QLoRA (Dettmers et al., 2023). QLoRA is an efficient parameter finetuning method for quantized LLMs, freezes the quantized weight and optimizes the float low-rank matrices, which is much similar to the original LoRA but takes lower memory. However, LoRA-Rounding only optimizes the rounding error of weight quantization, which is a much different method that is designed for post-training quantization with ultra-low cost.

3.4. Overall loss

In summary, by utilizing a low-rank decomposition of the weight-compensated matrix, we effectively reduce the number of learnable parameters S_W, S_X, A_1, A_2 while still achieving accurate correction of weight quantization errors within each block. The total loss for optimizing the i^{th} block to the k^{th} block within a sliding window is formulated as

$$\mathcal{L}_{total} = \mathcal{L}_{rec} + \gamma \mathcal{L}_{round}, \quad (10)$$

where the γ is the hyper-parameter to balance the reconstruction error and round error, which is set to 0.01 in our experiments. During optimization, We slide the window to the last block with an interval and update all the quantization parameters within the window, ensuring that the cumulative error in the quantized transformer block is minimized and achieves optimal performance.

4. Experiments

In this section, we conduct extensive experiments to validate the effectiveness and superiority of the proposed CBQ.

4.1. Setup

Models and datasets. We conduct experiments on large language models with different sizes, including OPT (Zhang et al., 2022) and LLAMA (Touvron et al.) families. We validate our quantization scheme on various datasets which are divided into two categories. One is reported by the perplexity metric of language generation experiments on C4 (Raffel et al., 2020) and WikiText2 (Merity et al., 2016). The other is reported by the accuracy metric of zero-shot language tasks on PIQA (Bisk et al., 2020a), HellaSwag (Clark et al., 2018), ARC (Clark et al., 2018), Mutual (Cui et al., 2020) and Ethics (Hendrycks et al., 2020a).

Quantization setting. To thoroughly evaluate performance, we test extensive quantization schemes including weight-only quantization down to W4A16 and W2A16, as well as joint weight-activation quantization for ultra-low bitwidths like W4A8, and W4A4. This extensive assessment across varying bitwidths provides a robust analysis of our proposed method. Also, with full consideration of the convenience of actual deployment of the quantized model, except for the settings with activation values below 4 bits that use per-token quantization, we perform per-tensor quantization on activations.

Baseline methods. For weight-only quantization settings, we selected GPTQ (Frantar et al., 2022b) as the baseline quantization method in our experiments. This represents the most prevalent technique for W4A16 quantization of language models, respectively. Furthermore, we compare our CBQ with OmniQuant (Shao et al., 2023) and QLLM (Liu et al., 2023), which is the state-of-the-art method based on block reconstruction. We include a comparison of our CBQ method with the groupwise quantization method RPTQ (Yuan et al., 2023), which is widely employed in the W4A8 setting.

Implementation details. Following the setting of previous work (Frantar et al., 2022b), our calibration dataset comprises 128 randomly selected 2048-token segments from C4 to ensure standardized benchmarking. To balance quantization performance and training speed, we utilize sliding windows containing two blocks with 3 epochs per window. For the LoRA-Rounding technique, we set the rank r to 5. The optimization process involves adjusting the learnable quantization step sizes (S_X and S_W) and the weight-rounding matrix (δ_W) with learning rates of $1e - 6$, $1e - 7$, and $1e - 4$, respectively. To manage the learning rate, we utilize the CosineAnnealingLR scheduler. We quantize all models using a mini-batch size of 1 on a single GPU. This configuration allows efficient cross-block dependency modeling while sufficiently propagating information across windows.

4.2. Experimental results

Evaluation on zero-shot datasets with accuracy. Results on multiple zero-shot benchmarks using accuracy as the evaluation metric demonstrate CBQ’s capabilities on large models including OPT (30B, 66B) and LLAMA (30B, 65B) (as shown in Table 1). Across almost all public datasets, CBQ outperforms existing quantization methods by over 2% and reduces the accuracy gap with the full precision model to within 1% under the W4A16, W2A16 and W4A8 quantization settings. This demonstrates stronger zero-shot capability. Moreover, unlike current techniques, CBQ uniquely achieves ultra-low quantization down to W4A4 bitwidths while maintaining a higher performance than the state-of-

#Num of blocks	w/ Overlap	C4↓	Wiki↓
1	✗	14.57	11.98
	✓	14.23	11.35
2	✗	13.29	10.63
	✓	14.32	11.45
4	✗	13.27	10.60
	✓		

Table 3. Ablation of the cross-block dependency (CBD).

Method	C4↓	Wiki↓
w/o outlier pre-processing	1082.68	1128.33
w/ Smoothquant (Xiao et al., 2022)	33.21	25.26
w/ CFP-Activation	23.48	19.75
w/ CFP-Weight + CFP-Activation	21.98	17.95
w/ Smoothquant + CBQ-Recon.	15.69	12.24
w/ CFP-Weight + CFP-Activation + CBQ-Recon.	13.29	10.63

Table 4. Ablation on the coarse-to-fine pre-processing. ‘CBQ-Recon.’ represents the proposed cross block reconstruction.

the-arts. The consistent gains verify the generalization of CBQ’s innovations across models and datasets.

Evaluation on generation datasets with perplexity. Results in Table 2 demonstrate our method’s generation performance on C4, WikiText2 using weight-only quantized OPT and LLAMA models. Focusing on ultra-low bitwidths, we achieve over 1% higher perplexity versus GPTQ at W4A16. These consistent improvements at low bitwidths highlight our advantages in preserving generative quality under aggressive compression rates.

Comparison of block reconstruction-based methods. We provide a comprehensive validation of the superiority of our proposed CBQ method compared to the state-of-the-art block reconstruction-based methods, OmniQuant and QLLM. To evaluate the performance improvement, we conducted experiments that encompassed multiple zero-shot tasks and generation tasks. The results, as presented in Table 1 and Table 2, consistently demonstrate the significant performance gains achieved by our CBQ method.

4.3. Ablation Study

To analyze the contribution of each component in our proposed CBQ method, we performed ablation experiments on the LLAMA-7B model.

Cross-block dependency. To analyze the impact of our proposed cross-block dependency (CBD) method, we per-

Method	PPL ↓			
	C4	Wiki	#Epochs	GPU (GB)
w/o Rounding	14.32	11.46	3	18.83
w/ Rounding	13.86	10.98	3	27.73
w/ Rounding	13.58	10.72	6	27.73
w/ LoRA-Rounding	13.29	10.63	3	21.01

Table 5. Ablation of the LoRA-Rounding.

formed ablation experiments in Table 3. Results demonstrate performance gains as the number of blocks jointly processed per sliding window increases, validating CBD’s ability to model inter-block dependencies. Furthermore, utilizing overlapping blocks between adjacent sliding windows supplements cross-window relational representation. This redundancy helps capture nuanced block interactions and enables additional accuracy improvements. Overall, these ablation studies highlight the benefits of CBD for progressively accumulating and propagating cross-block knowledge during CBQ optimization.

LoRA-Rounding. As shown in Table 5, the incorporation of the LoRA-Rounding technique into the learning process effectively mitigates the rounding errors that typically arise from weight quantization. This improvement leads to a significant enhancement in quantization accuracy. In comparison to the conventional ‘Rounding’ technique, our LoRA-Rounding approach utilizes low-rank decomposition to reduce the number of learnable parameters. This reduction not only reduces GPU memory consumption during training but also improves training speed. Despite the additional training costs, LoRA-Rounding significantly outperforms ‘Rounding’ in terms of performance.

Coarse-to-fine pre-processing. Ablation of the proposed coarse-to-fine pre-processing verifies performance improvements from suppressing outlier values before quantization, as shown in Table 4. Detecting and dynamic scaling extreme activation outliers reduces distortions, while additional truncating of weight outliers further stabilizes training. This tailored preprocessing stabilizes the data distribution for robust optimization at ultra-low bitwidths. It is important to note that this two-pronged pre-processing method is specifically designed to address the abundance of outliers in language models, which are not adequately addressed by the existing pre-processing technique of Smoothquant (Xiao et al., 2022). Furthermore, we conduct a reconstruction optimization process, referred to as ‘CBQ-Recon.’, based on the pre-processed weights and activations. This approach, compared to the optimization based on the processing of Smoothquant, yields better performance.

KL loss	L2 loss	Homologous	C4	Wiki
✗	✓	✗	13.82	11.13
✓	✗	✗	13.84	11.12
✓	✓	✗	13.55	10.88
✓	✓	✓	13.29	10.63

Table 6. Ablation study on block-wise reconstruction loss functions. ‘homologous’ represents the homologous reconstruction.

LLAMA	7B	13B	30B	65B
OmniQuant	1.6h	3.3h	7.3h	14.4h
QLLM*	1.05	1.79	-	9.05
CBQ	0.9h	1.45	2.1h	4.3h

Table 7. Comparison of training (GPU Hours) time of our CBQ with OmniQuant. * represents that the training time of QLLM is implemented on LLAMA2 models.

Loss functions. To determine optimal loss formulations, we evaluate reconstruction errors using L2 alone, KLD alone, and a combination of them in Table 6. Ablation results demonstrate superior performance from KLD over L2, with the combined loss achieving further gains. This highlights the benefits of KLD for matching full-precision block distributions during CBQ optimization. Fusing both losses enables jointly minimizing absolute and divergence-based errors to improve overall block-wise reconstruction. Our analysis verifies the advantage of blended L2+KLD loss for robustly optimizing blocks as interdependent components. Moreover, the introduced homologous reconstruction scheme further reduces the reconstruction difficulty and improves the quantization performance.

Comparison of quantization efficiency. We evaluate the quantization efficiency of our CBQ method and compare it to OmniQuant and QLLM, both of which are reconstruction-based PTQ methods. The GPU training hours for both methods are shown in Table 7. The results demonstrate that the training cost of CBQ can be faster than OmniQuant, particularly for larger models. This indicates that our CBQ method offers an advantage in terms of training efficiency.

5. Conclusion

In this study, we introduce CBQ, a unified post-training quantization method specifically designed for large language models. By jointly optimizing weight and activation quantization parameters through block-wise reconstruction, CBQ achieves efficient quantization without hand-craft searching. The introduced cross-block dependency scheme, low-rank decomposition scheme, and outlier detection strategy further improve the quantization performance. Experimental results demonstrate the state-of-the-art per-

formance of CBQ, particularly in ultra-low bit settings like W4A4 and W2A16, and better maintain the capability of the full-precision model in W4A8 and W4A16 settings. The proposed CBQ method contributes to advancing PTQ techniques for LLMs, paving the way for efficient and effective deployment of large language models in resource-constrained devices.

6. Acknowledgement

We gratefully acknowledge the support of MindSpore, CANN (Compute Architecture for Neural Networks) and Ascend AI Processor used for this research.

References

Bisk, Y., Zellers, R., Gao, J., Choi, Y., et al. Pixa: Reasoning about physical commonsense in natural language. In *Proceedings of the AAAI conference on artificial intelligence*, volume 34, pp. 7432–7439, 2020a.

Bisk, Y., Zellers, R., Le bras, R., Gao, J., and Choi, Y. Pixa: Reasoning about physical commonsense in natural language. *Proceedings of the AAAI Conference on Artificial Intelligence*, pp. 7432–7439, Jun 2020b. doi: 10.1609/aaai.v34i05.6239. URL <http://dx.doi.org/10.1609/aaai.v34i05.6239>.

Brown, T., Mann, B., Ryder, N., Subbiah, M., Kaplan, J., Dhariwal, P., Neelakantan, A., Shyam, P., Sastry, G., Askell, A., Agarwal, S., Herbert-Voss, A., Krueger, G., Henighan, T., Child, R., Ramesh, A., Ziegler, D., Wu, J., Winter, C., Hesse, C., Chen, M., Sigler, E., Litwin, M., Gray, S., Chess, B., Clark, J., Berner, C., McCandlish, S., Radford, A., Sutskever, I., and Amodei, D. Language models are few-shot learners. *arXiv: Computation and Language, arXiv: Computation and Language*, May 2020.

Cai, Y., Yao, Z., Dong, Z., Gholami, A., Mahoney, M. W., and Keutzer, K. Zeroq: A novel zero shot quantization framework. In *2020 IEEE/CVF Conference on Computer Vision and Pattern Recognition (CVPR)*, Jun 2020. doi: 10.1109/cvpr42600.2020.01318. URL <http://dx.doi.org/10.1109/cvpr42600.2020.01318>.

Choi, J., Chuang, P. I.-J., Wang, Z., Venkataramani, S., Srinivasan, V., and Gopalakrishnan, K. Bridging the accuracy gap for 2-bit quantized neural networks (qnn). *arXiv preprint arXiv:1807.06964*, 2018.

Clark, P., Cowhey, I., Etzioni, O., Khot, T., Sabharwal, A., Schoenick, C., and Tafjord, O. Think you have solved question answering? try arc, the ai2 reasoning challenge. *arXiv preprint arXiv:1803.05457*, 2018.

Cui, L., Wu, Y., Liu, S., Zhang, Y., and Zhou, M. Mutual: A

dataset for multi-turn dialogue reasoning. *arXiv preprint arXiv:2004.04494*, 2020.

Dettmers, T., Lewis, M., Belkada, Y., Zettlemoyer, L., and Paris-Saclay, E. Llm.int8(): 8-bit matrix multiplication for transformers at scale.

Dettmers, T., Pagnoni, A., Holtzman, A., and Zettlemoyer, L. Qlora: Efficient finetuning of quantized llms. *arXiv preprint arXiv:2305.14314*, 2023.

Frantar, E. and Alistarh, D. Optimal brain compression: A framework for accurate post-training quantization and pruning. Aug 2022.

Frantar, E., Ashkboos, S., Hoefer, T., and Alistarh, D. Gptq: Accurate post-training quantization for generative pre-trained transformers. Oct 2022a.

Frantar, E., Ashkboos, S., Hoefer, T., and Alistarh, D. Gptq: Accurate post-training quantization for generative pre-trained transformers. *arXiv preprint arXiv:2210.17323*, 2022b.

Han, S., Mao, H., and Dally, W. J. Deep compression: Compressing deep neural networks with pruning, trained quantization and huffman coding. *arXiv preprint arXiv:1510.00149*, 2015.

Hendrycks, D., Burns, C., Basart, S., Critch, A., Li, J., Song, D., and Steinhardt, J. Aligning ai with shared human values. *arXiv preprint arXiv:2008.02275*, 2020a.

Hendrycks, D., Burns, C., Basart, S., Zou, A., Mazeika, M., Song, D., and Steinhardt, J. Measuring massive multitask language understanding. *Cornell University - arXiv, Cornell University - arXiv*, Sep 2020b.

Hinton, G., Vinyals, O., and Dean, J. Distilling the knowledge in a neural network. *arXiv preprint arXiv:1503.02531*, 2015.

Hu, E. J., Shen, Y., Wallis, P., Allen-Zhu, Z., Li, Y., Wang, S., Wang, L., and Chen, W. Lora: Low-rank adaptation of large language models. *arXiv preprint arXiv:2106.09685*, 2021.

Hubara, I., Nahshan, Y., Hanani, Y., Banner, R., and Soudry, D. Improving post training neural quantization: Layer-wise calibration and integer programming. *arXiv preprint arXiv:2006.10518*, 2020.

Hubara, I., Nahshan, Y., Hanani, Y., Banner, R., and Soudry, D. Accurate post training quantization with small calibration sets. *International Conference on Machine Learning, International Conference on Machine Learning*, Jul 2021.

Kullback, S. and Leibler, R. A. On information and sufficiency. *The annals of mathematical statistics*, 22(1): 79–86, 1951.

Langley, P. Crafting papers on machine learning. In Langley, P. (ed.), *Proceedings of the 17th International Conference on Machine Learning (ICML 2000)*, pp. 1207–1216, Stanford, CA, 2000. Morgan Kaufmann.

Laurençon, H., Saulnier, L., Wang, T., Akiki, C., Moral, A., Scao, T., Werra, L., Mou, C., Ponferrada, E., Nguyen, H., Frohberg, J., Šaško, M., Lhoest, Q., Mcmillan-Major, A., Dupont, G., Biderman, S., Rogers, A., Allal, L., Toni, F., Pistilli, G., Nguyen, O., Nikpoor, S., Masoud, M., Colombo, P., Rosa, J., Villegas, P., Thrush, T., Longpre, S., Nagel, S., Weber, L., Muñoz, M., Zhu, J., Strien, D., Alyafeai, Z., Almubarak, K., Chien, V., Gonzalez-Dios, I., Soroa, A., Lo, K., Dey, M., Suarez, P., Gokaslan, A., Bose, S., Adelani, D., Phan, L., Tran, H., Yu, I., Pai, S., Chim, J., Lepercq, V., Ilić, S., Mitchell, M., Luccioni, S., and Jernite, Y. The bigscience roots corpus: A 1.6tb composite multilingual dataset. *Le Centre pour la Communication Scientifique Directe - HAL - Diderot, Le Centre pour la Communication Scientifique Directe - HAL - Diderot*, Nov 2022.

Li, Y., Gong, R., Tan, X., Yang, Y., Hu, P., Zhang, Q., Yu, F., Wang, W., and Gu, S. Brecq: Pushing the limit of post-training quantization by block reconstruction. *arXiv preprint arXiv:2102.05426*, 2021.

Lin, J., Tang, J., Tang, H., Yang, S., Dang, X., and Han, S. Awq: Activation-aware weight quantization for llm compression and acceleration. *arXiv preprint arXiv:2306.00978*, 2023.

Liu, J., Gong, R., Wei, X., Dong, Z., Cai, J., and Zhuang, B. Qllm: Accurate and efficient low-bitwidth quantization for large language models. *arXiv preprint arXiv:2310.08041*, 2023.

Liu, Z., Wang, Y., Han, K., Zhang, W., Ma, S., and Gao, W. Post-training quantization for vision transformer. *Advances in Neural Information Processing Systems*, 34: 28092–28103, 2021.

Merity, S., Xiong, C., Bradbury, J., and Socher, R. Pointer sentinel mixture models. *arXiv preprint arXiv:1609.07843*, 2016.

Nagel, M., Amjad, R. A., Van Baalen, M., Louizos, C., and Blankevoort, T. Up or down? adaptive rounding for post-training quantization. In *International Conference on Machine Learning*, pp. 7197–7206. PMLR, 2020.

Nagel, M., Fournarakis, M., Amjad, R. A., Bondarenko, Y., Van Baalen, M., and Blankevoort, T. A white paper on neural network quantization. *arXiv preprint arXiv:2106.08295*, 2021.

Park, G., Park, B., Kwon, S. J., Kim, B., Lee, Y., and Lee, D. nuqmm: Quantized matmul for efficient inference of large-scale generative language models. *arXiv preprint arXiv:2206.09557*, 2022.

Radford, A., Wu, J., Child, R., Luan, D., Amodei, D., and Sutskever, I. Language models are unsupervised multitask learners.

Raffel, C., Shazeer, N., Roberts, A., Lee, K., Narang, S., Matena, M., Zhou, Y., Li, W., and Liu, P. J. Exploring the limits of transfer learning with a unified text-to-text transformer. *The Journal of Machine Learning Research*, 21(1):5485–5551, 2020.

Shao, W., Chen, M., Zhang, Z., Xu, P., Zhao, L., Li, Z., Zhang, K., Gao, P., Qiao, Y., and Luo, P. Omnipoint: Omnidirectionally calibrated quantization for large language models. *arXiv preprint arXiv:2308.13137*, 2023.

Touvron, H., Lavril, T., Izacard, G., Martinet, X., Lachaux, M.-A., Lacroix, T., Rozière, B., Goyal, N., Hambro, E., Azhar, F., Rodriguez, A., Joulin, A., Grave, E., and Lample, G. Llama: Open and efficient foundation language models.

Tu, Z., Ma, J., Xia, T., Zhao, W., Ren, P., and Zheng, N. Caq: Context-aware quantization via reinforcement learning. In *2021 International Joint Conference on Neural Networks (IJCNN)*, pp. 1–8, 2021. doi: 10.1109/IJCNN52387.2021.9534248.

Wei, J., Tay, Y., Bommasani, R., Raffel, C., Zoph, B., Borgeaud, S., Yogatama, D., Bosma, M., Zhou, D., Metzler, D., Chi, E., Hashimoto, T., Vinyals, O., Liang, P., Dean, J., and Fedus, W. Emergent abilities of large language models. Jun 2022a.

Wei, X., Zhang, Y., Zhang, X., Gong, R., Zhang, S., Zhang, Q., Yu, F., and Liu, X. Outlier suppression: Pushing the limit of low-bit transformer language models. *Advances in Neural Information Processing Systems*, 35:17402–17414, 2022b.

Wei, X., Zhang, Y., Li, Y., Zhang, X., Gong, R., Guo, J., and Liu, X. Outlier suppression+: Accurate quantization of large language models by equivalent and optimal shifting and scaling. *arXiv preprint arXiv:2304.09145*, 2023.

Xiao, G., Lin, J., Seznec, M., Demouth, J., and Han, S. Smoothquant: Accurate and efficient post-training quantization for large language models. Nov 2022.

Yao, Z., Yazdani Aminabadi, R., Zhang, M., Wu, X., Li, C., and He, Y. Zeroquant: Efficient and affordable post-training quantization for large-scale transformers. *Advances in Neural Information Processing Systems*, 35: 27168–27183, 2022.

Yuan, Z., Niu, L., Liu, J., Liu, W., Wang, X., Shang, Y., Sun, G., Wu, Q., Wu, J., and Wu, B. Rptq: Reorder-based post-training quantization for large language models. *arXiv preprint arXiv:2304.01089*, 2023.

Zhang, S., Roller, S., Goyal, N., Artetxe, M., Chen, M., Chen, S., Dewan, C., Diab, M., Li, X., Lin, V., Mihaylov, T., Ott, M., Shleifer, S., Shuster, K., Simig, D., Koura, S., Sridhar, A., Wang, T., and Zettlemoyer, L. Opt: Open pre-trained transformer language models.

Zhang, S., Roller, S., Goyal, N., Artetxe, M., Chen, M., Chen, S., Dewan, C., Diab, M., Li, X., Lin, X. V., et al. Opt: Open pre-trained transformer language models. *arXiv preprint arXiv:2205.01068*, 2022.

Zoph, B. and Le, Q. Neural architecture search with reinforcement learning. *International Conference on Learning Representations, International Conference on Learning Representations*, Nov 2016.

A. Appendix

A.1. Overview

Method	Quantize W/A	Gradient-Based	Cross-Block Dependency	Weight Outlier	Activation Outlier	Rounding Error
GPTQ (Frantar et al., 2022b)	✓/✗	✗	✗	✗	✗	✗
RPTQ (Yuan et al., 2023)	✓/✓	✗	✗	✗	✓	✗
OS+ (Wei et al., 2023)	✓/✓	✗	✗	✗	✓	✗
SmoothQuant (Xiao et al., 2022)	✓/✓	✗	✗	✗	✓	✗
OmniQuant (Shao et al., 2023)	✓/✓	✓	✗	✓	✓	✗
QLLM (Liu et al., 2023)	✓/✓	✓	✗	✗	✓	✗
CBQ (Ours)	✓/✓	✓	✓	✓	✓	✓

Table 8. Comparison of different quantization methods for LLMs.

In Table 8, we compare the designed components of our CBQ with the existing quantization methods for LLMs. We can observe a comparison of the different components incorporated in various quantization methods LLMs. Our proposed CBQ method stands out by including multiple essential components to address the challenges associated with LLM quantization.

Firstly, CBQ ensures that both weight and activation values are quantized to improve computational efficiency and reduce memory requirements. This aligns with the requirements of other methods such as RPTQ, OS+, and SmoothQuant, and is different from GPTQ. Additionally, CBQ incorporates a gradient-based optimization approach, allowing for efficient optimization during the quantization process. This component is also present in OmniQuant and QLLM, signifying its significance in achieving accurate quantization results. Furthermore, CBQ introduces the cross-block dependency (CBD) component, enabling the modeling of long-range dependencies between adjacent blocks. This ensures better information flow and integration across multiple blocks, surpassing the capabilities of other methods such as OmniQuant and QLLM. Moreover, CBQ addresses the presence of weight and activation outliers, which can significantly impact the quantization process. By effectively handling these outliers, CBQ surpasses the capabilities of OS+, SmoothQuant, OmniQuant, and QLLM, which either do not consider or only partially address this issue. Lastly, CBQ accounts for rounding errors, a critical aspect of quantization. By incorporating a rounding error reduction scheme, CBQ ensures more accurate and reliable quantization results. This component is absent in all other compared methods.

In summary, our CBQ method outperforms existing quantization methods for LLMs by incorporating a comprehensive set of components that collectively address the challenges associated with LLM quantization. These components work synergistically to enhance the precision, accuracy, and efficiency of the quantization process, making CBQ a promising approach for LLM quantization.

A.2. Evaluation quantization for a series of OPT models

	#Bits	Methods	OPT-1.3B	OPT-2.7B	OPT-6.7B	OPT-13B
C4	FP	-	14.72	13.16	11.74	11.20
	W4A16	GPTQ CBQ	15.57 15.42	13.75 13.56	12.15 11.92	11.36 11.29
	W2A16	OmniQuant CBQ	27.33 15.99	19.16 13.83	15.44 12.19	14.16 11.52
Wikitext2	FP	-	14.62	12.47	10.86	10.12
	W4A16	GPTQ CBQ	15.56 15.10	12.82 13.58	11.41 11.10	10.31 10.24
	W2A16	OmniQuant CBQ	23.95 15.40	18.13 17.92	14.43 11.19	12.94 10.43

Table 9. Evaluation quantization for a series of OPT models on generation datasets with the perplexity \downarrow metric